Title
PPARγ Regulates Mouse Meibocyte Differentiation and Lipid Synthesis

Journal
The Ocular Surface, 14(4)

ISSN
1542-0124

Authors
Jester, James V
Potma, Eric
Brown, Donald J

Publication Date
2016-10-01

DOI
10.1016/j.jtos.2016.08.001

Peer reviewed

HHS Public Access

Author manuscript

Ocul Surf. Author manuscript; available in PMC 2017 October 01.

Published in final edited form as:

Ocul Surf. 2016 October ; 14(4): 484–494. doi:10.1016/j.jtos.2016.08.001.

PPARγ Regulates Mouse Meibocyte Differentiation and Lipid Synthesis

James V. Jester, PhD[1], **Eric Potma, PhD**[2], and **Donald J. Brown, PhD**[1]

[1]Gavin Herbert Eye Institute, University of California, Irvine, CA

[2]Department of Chemistry and Beckman Laser Institute, University of California, Irvine, Irvine, CA

Abstract

Purpose—Previous reports suggest that age-related meibomian gland atrophy is associated with decreased expression of the lipid sensitive nuclear receptor, PPARγ. The purpose of this study was to identify the role of PPARγ in modulating meibocyte lipid synthesis.

Methods—Cytoplasmic and nuclear fractions from meibomian glands of young (2M) and old (2Y) C57Bl6 mice were probed using antibodies specific for PPARγ. Mouse meibocytes were cultured, immortalized using a SV40 lentiviral vector, and evaluated for lipid synthesis using LipidTox staining and CARS/Raman microspectroscopy. Lipid synthesizing clones were tested for effects of PPARγ agonist, rosiglitazone, on lipid synthesis and PPARγ localization, post-translational modification and induction of PPARγ response genes.

Results—The cytoplasmic fraction in young mice contained both 50 and 72 kDa PPARγ bands that were absent or reduced by 75% in older mice, respectively. Cultured meibocytes produced neutral lipid containing equal amounts of wax and cholesterol esters, similar to mouse meibum. Addition of rosiglitazone (10–50 μM) significantly increased lipid production ($P<.05$) in meibocytes, associated with SUMO1 sumoylation and cytoplasmic accumulation of the 72 kDa PPARγ. Rosiglitazone also increased the localization of PPARγ to the cytoplasm and up-regulated of PPARγ, ADP and ADFP mRNA.

Conclusions—This study confirms the loss of cytoplasmic/vesicular PPARγ localization in older, atrophic mouse meibomian glands. Furthermore, PPARγ stimulates lipid synthesis in mouse meibocytes, associated with PPARγ sumoylation and translocation to the cytoplasm. Taken together these data suggest that lipid synthesis in older mice is down regulated by a PPARγ mediated pathway.

Keywords

eyelid; lipid; meibocytes; meibomian gland; PPARγ; tear film

Corresponding author: James V. Jester, PhD, Gavin Herbert Eye Institute, University of California Irvine, Hewitt Hall, 843 Health Sciences Road, Building 843, 2nd Floor, Irvine, CA 92697. Tel: 949-824-8047. jjester@uci.edu.

I. Introduction

Meibomian glands are lipid-excreting, holocrine glands that are embedded in the tarsal plate of the mammalian eyelid and provide lipid to the tear film.[1,2] Loss of tear film lipid is known to cause tear film instability, increase tear evaporation, and increase tear film osmolarity, causing an evaporative form of dry eye.[3–6] Evaporative dry eye is generally thought to be an age-related disorder that is a common clinical complaint of patients visiting the ophthalmologist or optometrist and may comprise from 37% to 47% of the average patient population.[7] Recently, there has been increasing awareness of the association between evaporative dry eye and meibomian gland dysfunction (**MGD**) in the form of meibomian gland dropout and altered lipid quantity and/or quality.[8–10]

While the risk of evaporative dry eye and MGD increases with age, much remains to be clarified regarding the underlying cellular and molecular mechanisms.[11] Past clinical and animal studies have established that meibomian glands are susceptible to keratinization and that genetic alterations and chemical agents, i.e., chlorinate biphenyls and epinephrine, can lead to replacement of the meibomian gland with keratic cysts.[12–14] These observations have formed the basis for an obstructive model of MGD where hyperkeratinization of the meibomian gland duct leading to ductal occlusion and plugging is thought to cause cystic dilation and a ‘disuse atrophy’ of the gland.[6] Androgens have also been implicated in the development of evaporative dry eye, based on findings that neutral and polar lipid profiles of meibomian glands show distinct differences related to sex and the presence of functional androgen receptors.[15,16] While keratinization and androgens are clearly important to gland function, the overall regulation of meibomian gland differentiation and lipid synthesis remains unknown.

Recently, a telomerase immortalized human meibomian gland epithelial cell line has been developed that has been used to evaluate the influence of androgens, growth factors, serum, neurotransmitters, and antibiotics on meibomian gland epithelial proliferation and lipid synthesis.[17–25] In these studies, gene expression analysis has shown that peroxisome proliferative activated receptor (**PPAR**) signaling can be differentially regulated based on induction of proliferation or differentiation. PPARs are a family of lipid-sensitive nuclear receptors that show distinct tissue localizations and physiologic activities. One member, PPARγ, has been shown to play an important role in regulating lipid synthesis and differentiation of adipocytes and sebocytes and is known to interact with other nuclear hormone receptors, including androgens and retinoic acid.[26–28] While past studies have shown that PPARγ is expressed in developing and adult mouse meibomian glands,[29] the role of PPARγ signaling on meibocyte lipid synthesis is not known.

Interestingly, during aging of humans and mouse meibomian glands, PPARγ undergoes a change in the immunocytochemical localization within meibocytes from a vesicular/cytoplasmic and nuclear localization in young glands to a predominantly nuclear pattern in older glands. This change occurs concurrently with decreased basal acinar cell proliferation, gland atrophy and clinically identified meibomian gland dropout.[30–32] Overall, these findings support the hypothesis that aging of the meibomian gland involves altered

meibocyte differentiation and PPARγ receptor signaling that is associated with meibomian gland dropout and altered lipid quality.

To test this hypothesis we have evaluated the subcellular localization of PPARγ in meibomian glands of young and old mice and cultured mouse meibocytes. In this paper we present data showing that the cytoplasm of meibocytes contain a 50/72 kDa PPARγ that is decreased or absent in meibomian glands from older mice. Furthermore, treatment of cultured mouse meibocytes with the PPARγ agonist, rosiglitazone, induces lipid synthesis coincident with sumoylation and increased localization of PPARγ to the cytoplasm along with up-regulation of PPARγ response genes. Taken together, these findings indicate that PPARγ regulates lipid synthesis in meibocytes and suggest that age-related atrophy of mouse meibomian glands involves downregulation of PPARγ-induced lipid synthesis.

II. Materials and Methods

A. Animals

C57Bl/6 mice were used in this study. All animal procedures were approved by the University of California, Irvine, Institutional Animal Care and Use Committee and were conducted in accordance with the ARVO Statement for the Use of Animals in Ophthalmic and Vision Research. All animals were humanely sacrificed by cervical neck dislocation following sedation with ketamine (100 mg/Kg body weight) and xylazine (20 mg/Kg body weight) prior to tissue collection.

B. Isolation, Culture, Immortalization and Characterization of Mouse Meibocytes

Isolation and Culture—The upper and lower eyelids of twenty 6-week-old mice were removed, disinfected with 70% ethanol and dissected using a Zeiss SteREO Discovery.V12 microscope (Carl Zeiss MicroImaging, LLC, United States). Tissues were first washed with phosphate buffer saline (PBS, pH 7.2) and then immediately placed in Dulbecco's modified Eagle's medium (DMEM) supplemented with antibiotics (Invitrogen, Carlsbad, CA). The conjunctiva and excess skin was removed and the tarsal plates carefully excised and placed in PBS containing 0.25% collagenase A (Invitrogen, Carlsbad, CA) and 0.6U/ml dispase II (Invitrogen). Glands were then digested at 37°C overnight followed by centrifugation at 1,500 RPM for 15 minutes. The cell pellet was then suspended in Keratinocyte Growth Medium (KGM, Lonza Walkersville, Inc., Walkersville, MD) containing human epidermal growth factor (**hEGF**), insulin (bovine), Hydrocortisone and antibiotics (Gentamicin) supplemented with 10% fetal bovine serum. Cells were cultured on 6-well primaria culture plates (Becton Dickinson and Company, Franklin Lakes, NJ) and maintained in a humidified 5% CO_2 incubator at 37°C. In the reported studies, 2 batches of mice were used to establish meibocyte cultures for characterizing lipid synthesis and immortalization, respectively.

Immortalization of Meibocytes—Primary mouse meibocytes at 40–50% confluence were immortalized using a SV40 large T-antigen inserted in a lentiviral vector (Applied Biological Materials Inc., Richmond, BC Canada). Briefly, viral supernatant containing 0.8 μg/ml of polybrene transfection reagent (Millipore Corporation, Phillisburg, NJ) was added to meibocytes cultures. Cells were then cultured overnight and the viral supernatant removed

and replaced by serum supplemented KGM complete growth medium for an additional 72 hours. Cells were then plated in 60-mm dishes at a limited dilution of 50 cells/dish. Single clones were then isolated using a cloning disc soaked with Trypsin-EDTA and subcultured to 6-well plates. Initially, 8 clones were isolated, and one clone (CN-G2) that produced abundant lipid droplets was selected for further study.

Characterization of Clone CN-G2—The lipid-producing clone, CN-G2, was characterized for the production of lipid and the effects of serum and PPARγ agonist, rosiglitazone. Cells at passage 23 and above were plated at 30% confluence in either glass chamber slides (BD Falcon 4-well CultureSlide, Rockville, MD) for immunocytochemistry and lipid staining or 100-mm diameter dishes for biochemical and RNA analysis. Cells were then cultured for 7 days (3 coverslips and 3 dishes per condition) in either 0%, 1%, 2% or 10% serum containing KGM growth media to determine the effects of serum on lipid synthesis and PPARγ localization. To assess the effects of rosiglitazone, cells were plated at 30% confluence in 2% serum containing KGM growth media for 7 days and then switched to media containing rosiglitazone at 10 μM, 20 μM and 50 μM (Enzo Life Sciences, Plymouth Meeting, PA) with changes in the media every other day. Cells were then collected at 1, 3, and 5 days (3 coverslips per condition) and 7 days (3 coverslips and 3 dishes per condition) for analysis of lipid synthesis or PPARγ localization and gene expression.

C. Immunocytochemistry

For analysis of meibomian glands, eyelids from 3 young (2-month-old) and 3 old (2-year-old) mice was initially fixed overnight in 2% paraformaldehyde in PBS at 4°C, washed in PBS, embedded in Tissue Tech O.C.T. Compound (Sakura Finetek USA, Inc, Torrance, CA), frozen in liquid nitrogen and stored at −80°C and then sectioned using a Leica CM1850 Cryotome (Leica, Wetzlar, Germany), and mounted onto glass slides. For analysis of cultured meibocytes, cells were fixed in 2% paraformaldehyde in PBS for 2 hours.

For immunostaining, cells and tissue sections were permeablized in PBS containing 0.5% dimethyl sulfoxide and 0.5% Triton X (pH 7.2) for 5 minutes and then washed in PBS. Slides were then incubated in goat serum (1/30) for 30 minutes at 37°C and then incubated with rabbit anti-PPARγ (1:50, Abcam, Cambridge, MA). Slides were then washed with PBS, stained with FITC conjugated goat anti-rabbit IgG (1:200, Invitrogen) for 1 hour at 37°C and then counterstained with DAPI (Invitrogen). For negative controls, primary antibodies were either omitted or replace by nonspecific rabbit sera. The samples were then evaluated and imaged using a Nikon Eclipse E600 epifluorescence microscope (Nikon Inc, Melville, NY).

D. Assessment of Meibocyte Lipid Synthesis

To assess whether immortalized meibocytes synthesized lipids characteristic of the meibomian gland, CN-G2 cells were evaluated by coherent anti-Stokes Raman scattering (CARS) and Raman microspectroscopy using previously published techniques.[33] Briefly, multimodal CARS microscopy was carried out using an inverted confocal microscope (Fluoview 300, Olympus) and an optical parametric oscillator (Levante Emerald OPO, APE, Berlin) pumped by the second harmonic of a Nd:vanadate picosecond mode-locked laser

(PicoTrain, High-Q). CARS images were obtained using a 20×, 0.70 NA objective (UplanSApo, Olympus), which has a ~0.5 μm lateral and ~3.5 μm axial focal volume. Raman microspectroscopy was carried out using a frequency doubled Nd:vanadate laser (Verdi V5, Coherent) tuned to 532 nm. Raman microspectroscopy was coupled to CARS through the back port of the microscope and used the same objective lens. Switching between CARS and Raman detection was accomplished using a carrousel, allowing detection of lipid droplets using CARS, which were then directly analyzed by Raman.

To measure the lipid content, cells were stained with neutral lipid fluorescent probe, HCS LipidTOX™ (Invitrogen. Carlsbad, CA). Cells were fixed in 2% paraformaldehyde and then rinsed in PBS. Cells were then incubated in HCS LipidTox solution (dilution 1:1000) for 20 minutes at room temperature. Coverslips were rinsed in PBS, counterstained with DAPI nuclear stain and fluorescence imaged using the Nikon Eclipse E600 microscope. A total of 5 random images for each coverslip (3 coverslips totaling 15 image per treatment) were digitized and then analyzed using Metamorph Image Processing Software (Molecular Devices, Downington, PA, USA). All coverslips from each experiment were stained and evaluated on the same day to reduce the effects of random variations in staining intensity and imaging. Regions of fluorescence were first thresholded using the Threshold subroutine to include all high intensity pixels representing lipid droplets within cells and generally included pixel intensities from 100 to 255. This threshold was then applied to all subsequent images taken during the same experiment. Thresholded pixel area was then measured using the *Measure* subroutine in Metamorph and the area recorded. For each image the number of cells was also determined by counting the nuclei using the Manual Count subroutine. To calculate the lipid content per cell in each image, the thresholded lipid pixel area was then divided by the total number of cells in each image.

E. Protein Isolation and Western Blotting

For mouse meibomian glands, 5 young (2-month-old) and 5 old (2-year-old) mice were sacrificed and the meibomian glands isolated from the upper and lower eyelids and pooled together to obtain enough protein for multiple western blots. Tissues were then homogenized using a Polytron (PT-1200, Kinematic, Bohemia, NY). For extraction of protein from tissue cultured cells, 100 mm dishes were first rinsed 3 times in Dulbecco's phosphate buffered saline, and then cells were scraped from the dish using a polyethylene Cell Lifter (Corning Inc., Corning, NY). Proteins from tissues and cells were fractionated using the NE-PER Nuclear & Cytoplasmic Extraction Reagent kit from Thermo Scientific (Rockford, IL). All extraction buffers were supplemented with the Calbiochem Protease Inhibitor Cocktail Set III (EMD Chemical Inc, Gibbstown, NJ) and Phosphatase Inhibitor Cocktail 2 (Sigma-Aldrich, St Louis, MO). The protein content of the cell and tissue extracts was then measured using the RC DC Protein Assay (Bio-Rad Laboratories, Hercules, CA) and the samples run on 12% SDS PAGE gels. Proteins were then transferred to PVDF membranes using iBlot Gel Transfer Device (Invitrogen, Carlsbad, CA). Membranes were then blocked using 5% non-fat dry milk in PBS-T (0.2% Tween 20) and then immunostained using antibodies to PPARγ (Dilution 1:500). Membranes were then rinsed with PBS-T and then incubated with goat anti-rabbit IgG (H+L) HRP (Dilution 1:2500; Invitrogen), rinsed with PBS-T and incubated with SuperSignal® West Pico Chemiluminescent Substrate (Thermo

Scientific, Rockford, IL). Immunostained bands were then detected using photographic film. All western blots were repeated 3 times.

F. Immunoprecipitation

Cytoplasmic extracts from cultured meibocytes were first immunopreciptated using goat anti-PPARγ antibodies (sc-22020, Santa Cruz Biotechnology, Dallas, TX) linked to Dynabeads-Protein G (Novex, Life Technologies, Oslo, Norway). Proteins were eluted and then western blotted using rabbit anti-PPARγ antibodies (ab27649, Abcam, Cambridge, MA) to identify presence of cytoplasmic 50 and 72 kDa PPARγ. Blots were then stripped using a mild stripping protocol and then reacted with rabbit monoclonal antibody to SUMO1 (ab133352, Abcam).

G. RNA Isolation and Analysis of Gene Expression

Gene expression was evaluated by real time PCR using previously published methods.[34, 35] Briefly, cells were directly lysed using RLT buffer and the RNA isolated over RNeasy spin columns as suggested by the manufacturer (Quiagen, Valencia CA). RNA yield and quality was evaluated with the aid of a Nanodrop spectrophotometer (Thermo Scientific, Wilmington,DE). 0.5 μg RNA was reverse transcribed using oligo dT and random primers as supplied in the QuantiTect Reverese Transcription Kit (Quiagen). Real time PCR was performed using Power Sybr Green reagents (ABI Life Technologies, Foster City, CA) and validated real time PCR primers obtained from SA Biosciences (Quiagen). Products were evaluated by melt curve analysis and sizing on agarose gels. Relative quantization was performed using the delta delta C_T method using both GAPDH and beta actin as the normalizing housekeeper genes as previously described.[34]

H. Statistical Analysis

All results are reported as mean ± standard deviation. Differences between groups were assessed by one-way ANOVA and Bonferroni multiple comparisons (Sigma Stat version 3.11, Systat Software Inc, Point Richmond, CA). All experiments were repeated at least 3 times.

III. Results

A. Cytoplasmic and Nuclear PPARγ Expression

As shown earlier,[31] immunostaining of mouse eyelids with antibodies specific for PPARγ show a cytoplasmic/vesicular and nuclear localization of PPARγ within the acinar cells of meibomian glands in young mice (Figure 1A). This is in contrast to the predominantly nuclear localization that is detected in acinar cells of meibomian glands in older mice (Figure 1B). Subcellular fractionation of pooled mouse meibomian gland tissue (5 mice/age group) into cytoplasmic and nuclear fractions showed that the nucleus contains almost exclusively a 50 kDa PPARγ in both young (2M) and old (2Y) glands that is consistent with the expression of the γ1 splice variant of PPARγ (Figure 1C).[36] Furthermore, staining of western blots with antibodies specific for γ1 showed positive staining while antibodies to γ2 failed to stain (data not shown). Evaluation of the cytoplasmic fraction showed that in addition to the 50 kDa PPARγ splice variant there was a 72 kDa PPARγ variant suggesting

post translational modification of PPARγ. Comparison of young (2M) and old (2Y) meibomian glands indicated that there was a marked decrease in both the 50 and 72 kDa PPARγ forms in the cytoplasmic compartment of the old meibomian glands, with almost complete loss of the 50 kDa PPARγ. Densitometry measurements based on normalization to GAPDH staining (Figure 1D) showed a significant (P<.05) 75% decrease in the 72 kDa band and complete loss for the 50 kDa band. Additionally, the nuclear 50 kDa PPARγ was reduced by 40% based on densitometry normalized to nuclear Histone 3 expression (H3).

B. Characterization of Immortalized Mouse Meibocytes

After immortalization and cloning, we compared the characteristics of primary cultured, normal mouse meibocytes to that of the SV40 transformed and immortalized mouse meibocyte clone, CN-G2 (Figure 2). Cultured normal mouse meibocytes showed an epithelial morphology with very slow growth that required weeks to come to confluence. In culture many cells showed accumulation of perinuclear vacuoles (Figure 2A) that appeared to enlarge over time. By contrast, CN-G2 immortalized cells were fast growing but also showed an epithelial morphology and the accumulation of perinuclear vacuoles that at times filled the cytoplasm (Figure 2B, arrows). Staining of cells with antibodies specific to PPARγ showed that both normal meibocytes (Figure 2C) and CN-G2 cells (Figure 2D) contained both nuclear and cytoplasmic localized PPARγ. Cytoplasmic staining was both diffuse and filamentous with some cells that contained perinuclear vacuoles, presumably representing lipid, showing strong diffuse PPARγ staining (Figure 2D, arrow). Staining of CN-G2 cells (Figure 2E) and normal meibocytes (data not shown) with the neutral lipid probe, LipidTox (Green), showed strong fluorescent staining of cytoplasmic vacuoles indicating the synthesis of neutral lipids. These fluorescent images were digitized and then thresholded using digital imaging software as shown in Figure 2F to measure lipid area

To verify that the cells were meibocytes and synthesized meibomian gland lipid, CN-G2 cells were analyzed using CARS and Raman spectroscopy. Cells that contained visible lipid droplets by brightfield microscopy showed the presence of bright spots using CARS imaging [Figure 3(a)]. In general, lipid droplets ranged in size from 1.3–4.0 μm in diameter, which is sufficiently large to probe with Raman spectroscopy. The spontaneous Raman spectrum that was obtained from the lipid droplets is shown in Figure 3(b); Red line = CN-G2 cells. For comparison, the Raman spectrum obtained from mouse meibomian gland lipid is also shown [Figure 3(b); Black line = MG Acini]. It should be noted that the two main peaks at 2846 cm^{-1} and 2886 cm^{-1} represent the respective symmetric and asymmetric CH_2 stretching vibrations of purified wax and cholesterol esters, characteristic of the major meibomian gland lipids that have been previously reported.[33] Importantly, the lipids synthesized by CN-G2 cells show similar peak vibrational components indicating the lipid contains high amounts of wax esters and cholesterol esters. By contrast, lipids from sebaceous gland and fat tissue, which have reduced cholesterol esters, show remarkably different Raman spectra with a reduced vibrational peak at 2886 cm^{-1} [Figure 3(c); Black = sebocyte and Blue = adipocyte]. Of interest was the finding that there is a third broad peak around 2940 cm−1 [Figure 3(b), arrow], which corresponds to a lower peak identified in the meibomian gland acinar lipid and represents a CH_3 stretch vibration associated with protein. This peak has

been shown to vary depending on the location of lipid from the acini to the duct, and may contain information regarding the protein content or lipid fluidity.[33]

C. Lipid Synthesis and PPARγ Localization in Cultured Meibocytes

Since serum contains unsaturated and essential free fatty acids, which are ligands for PPARγ, cells were cultured in different serum concentrations to evaluate the effects of serum on lipid synthesis. When cells were cultured for 7 days and then stained with LipidTox, there was a marked reduction in the neutral lipid staining in low serum concentrations compared to cells maintained in 10% serum (Figures 4A and 4B, respectively). Quantifying the amount of lipid present in cultures showed that there was a significant reduction ($P<.05$) in total lipid area/cell when cells were cultured in media contain 0%, 1% or 2% serum with an 82%, 83% and 37% reduction in lipid synthesis, respectively (Figure 4C). Although 2% serum containing media appeared to promote lipid synthesis compared to serum free or 1% serum, 2% serum maintained cell viability while at the same time significantly reducing lipid synthesis compared to 10% serum treated cultures. Reduced serum also altered the localization of PPARγ as identified by cell fractionation and western blotting (Figure 4D). While no change was detected in the localization of nuclear PPARγ, cultures grown in low serum showed a significant ($P<.05$) loss of the cytoplasmic 72 kDa PPARγ compared to cells grown in 10% serum containing media. Overall, these findings indicate that reduced serum concentrations in the culture media lead to significant loss of lipid synthesis that is associated with loss of the 72 kDa PPARγ protein.

D. Effects of Rosiglitazone on Lipid Synthesis and PPARγ Localization

CN-G2 cells were grown in media containing 2% serum for 7 days, and then treated with rosiglitazone, a member of the thiazolidineiones family of synthetic PPARγ agonists that has been shown to have important anti-type 2 diabetic actions.[28] It stimulates sebum production in diabetic patients and lipid synthesis in sebocyte cell cultures.[37] Cells treated for 7 days with rosiglitazone showed a significant ($P<.05$), dose- and time-dependent, 8–10-fold increase in lipid area per cell following exposure to 10 μM, 20 μM and 50 μM rosiglitazone when compared to baseline lipid levels (Figure 5). Fractionation of cells and western blotting for the cytoplasmic fraction of PPARγ after 7 days exposure to rosiglitazone (Figure 6A) also showed a significant ($P<.05$) dose-dependent increase in cytoplasmic PPARγ compared to untreated CN-G2 cells (0 μM). Interestingly, cytoplasmic fractions from CN-G2 cells also showed increased amounts of both the 50 kDa and 72 kDa PPARγ protein with the appearance of multiple bands. These additional bands most likely represent post translational modifications involving serine phosphorylation and sumoylation. To identify whether these higher molecular weight bands were due to post-translational modification of PPARγ, the cytoplasmic fraction was immunoprecipitated to isolate PPARγ using a goat anti-PPARγ antibody (Figure 6B). Staining of western blots with rabbit anti-PPARγ confirmed the immunoprecipitation of both the 50 kDa and 72 kDa PPARγ bands (Lane 1). Stripping and reprobing of western blots with antibodies against SUMO1 showed that the 72 kDa PPARγ band was sumolyated and post translationally modified (Lane 2). RNA extracted from cultures treated with 50 μM rosiglitazone also showed enhanced expression of PPARγ, adiponectin and ADFP (Figure 6C, number above bar = range) as measured by real-time PCR.

IV. Discussion

This report establishes that aging in the mouse meibomian gland leads to a loss in the expression of the lipid-sensitive nuclear receptor, PPARγ, with complete loss of the 50 kDa PPARγ1 splice variant and substantial loss of a 72 kDa PPARγ band within the cytoplasmic compartment of the gland. Cell culture studies using an SV40 transformed meibocyte cell line also confirm that decreased lipid synthesis associated with reduced serum concentrations was associated with loss of the 72 kDa PPARγ. Furthermore, this report establishes for the first time that the PPARγ agonist, rosiglitazone, dose-dependently increases lipid synthesis concomitant with increased PPARγ cytoplasmic localization of both the 50 kDa and 72 kDa proteins, identifies the sumolyation of PPARγ by SUMO1 as potentially playing a role in nuclear export of PPARγ, and establishes the upregulation of PPARγ response genes involved in lipid synthesis, i.e. adiponectin and ADFP. Taken together, these findings suggest that lipid synthesis in the meibomian gland is regulated by PPARγ and that during aging there is decreased PPARγ receptor activation, leading to deceased lipid synthesis and age-related atrophy of the meibomian gland.

Past studies have shown that the human meibomian glands undergo age-related changes similar to that identified in the mouse, including a loss of cytoplasmic localization of PPARγ and decreased acinar cell proliferation in older individuals.[30] These findings, taken together with our cell culture findings showing that loss of cytoplasmic PPARγ is associated with significantly decreased lipid synthesis, suggest that aging in humans leads to decreased lipid synthesis. Importantly, the changes in PPARγ in human lids, while significantly correlated with age, also show significant correlations with the development of MGD as graded by the quality of the lipid expression and gland dropout.[30] Since age was the only significant predictor of the change in PPARγ localization in our recently published study,[30] it is likely that decreased lipid synthesis and gland atrophy precede the development of age-related MGD. While these cell culture and biochemical findings need to be repeated and confirmed in humans, overall they suggest that loss of PPARγ signaling and downregulation of lipid synthesis leading to meibomian gland atrophy may be a major cause of evaporative dry eye in older patients. Clearly, understanding the role of PPARγ in meibomian gland function may provide important insights into understanding the development of age-related MGD and provide novel approaches to treating this disease.

As shown, meibomian glands express the γ1 isoform of PPARγ, which is a 475 aa alternative splice variant of PPARγ lacking the N-terminal 30-residues.[36] PPARγ1 contains an N-terminal transactivation domain (residues 30–136 of the full length transcript), a DNA-binding domain (residues 136–140), and a C-terminal ligand-binding domain (residues 204–505) having ligand-dependent transactivation function. PPARγ1 also contains a consensus serine phosphorylation site at S112[38, 39] and two sumoylation sites, K107 and K395.[40] Growth up-regulation through MAP kinases have been shown to lead to phosphorylation of PPARγ at S112 followed by sumoylation by SUMO1 or 2/3 at K107/K395, leading to increased transcriptional activity, cytoplasmic transport, and other unknown downstream effects involved in cell differentiation and lipid synthesis.[41,42] Our finding of a 72 kDa PPARγ protein within the cytoplasmic compartment of lipid synthesizing meibocytes and young meibomian glands suggests that post-transcriptional modification including serine

phosphorylation and sumoylation of PPARγ plays an important role in regulating lipid synthesis within meibocytes. The finding that the PPARγ agonist, rosiglitazone, induces post translational modification of PPARγ by SUMO1 and the cytoplasmic localization of PPARγ while stimulating lipid synthesis, further supports this hypothesis. In future studies it will be important to establish the role of PPARγ sumoylation and its role in regulating meibocyte differentiation. Nevertheless, the finding the PPARγ agonists stimulate lipid synthesis suggests that these agents may have potential therapeutic effects in restoring lipid synthesis in meibomian glands of patients suffering age-related MGD.

For this study, we immortalized mouse meibocytes using an SV40 viral vector. While transformation using viral oncogenes are known to produce cell lines showing genetic instability and altered cell growth regulation and differentiation, a similar approach has been used for the sebaceous gland to establish a lipid synthesizing cell line for which the molecular mechanisms of sebaceous gland function have been evaluated.[43–46] Recently, a human telomerase immortalized meibomian gland epithelial cell line has been generated that contains neutral lipids, expresses genes involved in lipid synthesis and responds to androgens.[21] Since telomerase immortalization has been shown to maintain normal cell differentiation,[47] future studies are needed to compare our findings regarding regulation of lipid synthesis by PPARγ in this meibomian gland epithelial cell line. Additionally, the effects of androgens, known to play an important role in the development of MGD in patients, on PPARγ signaling are also needed.

Finally, Raman spectral analysis of CN-G2 lipid detected an elevated vibrational peak around 2940 cm^{-1} in addition to the two main peaks at 2846 cm^{-1} and 2886 cm^{-1} associated with wax and cholesterol esters. Though less prominent, this peak was also identified in the mouse meibomian gland acinar lipid and showed progressive decreasing levels as lipid moved from the acinus to the central meibomian gland duct suggesting maturation of the lipid.[33] The significance of this peak is possibly related to either increased protein associated with the lipid or differences in lipid fluidity. The finding that CN-G2 cells show an enhanced vibrational peak in this region is consistent with this maturation hypothesis; newly synthesized meibomian gland lipid would contain the highest amount of associated protein or change in fluidity. Further study is needed to determine the significance of this region and whether lipid produced by meibocytes in culture undergoes similar maturation following synthesis of lipid.

V. Conclusion

This study shows that lipid synthesis in the mouse is regulated by the lipid-sensitive nuclear receptor, PPARγ. Furthermore, downregulation of lipid synthesis by serum starvation leads to decreased cytoplasmic localization of PPARγ in cultured meibocytes, similar to that observed in older mice and human meibomian glands. Taken together, these findings suggest that there is an age-related decrease in lipid synthesis by the meibomian gland that may explain, in part, age-related MGD and the development of evaporative dry eye in this patient population.

Acknowledgments

The authors wish to recognize and thank Chyong Jy Nien, MD, Salina Massei, Gloria Lin, Ginna Kim, and Tejas Shah who have provided assistance in the collection and analysis of the data presented in this paper.

Supported by NEI EY021510, The Skirball Program in Molecular Ophthalmology and Research to Prevent Blindness, Inc., Unrestricted Grant.

References

1. Bron, AJ.; Tripathi, RC.; Tripathi, BJ. Wolff's Anatomy of the Eye and Orbit. 8th. London: Chapman & Hall Medcial; 1997.
2. Jester JV, Nicolaides N, Smith RE. Meibomian gland studies: histologic and ultrastructural investigations. Invest Ophthalmol Vis Sci. 1981; 20:537–547. [PubMed: 7194327]
3. Mishima S, Maurice DM. The oily layer of the tear film and evaporation from the corneal surface. Exp Eye Res. 1961; 1:39–45. [PubMed: 14474548]
4. Mathers WD, Lane JA. Meibomian gland lipids, evaporation, and tear film stability. Adv Exp Med Biol. 1998; 438:349–360. [PubMed: 9634908]
5. Gilbard JP, Rossi SR, Heyda KG. Tear film and ocular surface changes after closure of the meibomian gland orifices in the rabbit. Ophthalmology. 1989; 96:1180–1186. [PubMed: 2797721]
6. Foulks GN, Bron AJ. Meibomian gland dysfunction: a clinical scheme for description, diagnosis, classification, and grading. Ocul Surf. 2003; 1:107–126. [PubMed: 17075643]
7. Lemp MA, Nichols KK. Blepharitis in the United States 2009: a survey-based perspective on prevalence and treatment. Ocul Surf. 2009; 7:S1–S14. [PubMed: 19383269]
8. Tong L, Chaurasia SS, Mehta JS, Beuerman RW. Screening for meibomian gland disease: its relation to dry eye subtypes and symptoms in a tertiary referral clinic in singapore. Invest Ophthalmol Vis Sci. 2010; 51:3449–3454. [PubMed: 20181848]
9. Viso E, Gude F, Rodriguez-Ares MT. The association of meibomian gland dysfunction and other common ocular diseases with dry eye: a population-based study in Spain. Cornea. 2011; 30:1–6. [PubMed: 20847672]
10. Nichols KK, Foulks GN, Bron AJ, et al. The international workshop on meibomian gland dysfunction: executive summary. Invest Ophthalmol Vis Sci. 2011; 52:1922–1929. [PubMed: 21450913]
11. Knop E, Knop N, Millar T, et al. The international workshop on meibomian gland dysfunction: report of the subcommittee on anatomy, physiology, and pathophysiology of the meibomian gland. Invest Ophthalmol Vis Sci. 2011; 52:1938–1978. [PubMed: 21450915]
12. Jester JV, Nicolaides N, Kiss-Palvolgyi I, Smith RE. Meibomian gland dysfunction. II. The role of keratinization in a rabbit model of MGD. Invest Ophthalmol Vis Sci. 1989; 30:936–945. [PubMed: 2470694]
13. Jester JV, Rajagopalan S, Rodrigues M. Meibomian gland changes in the rhino (hrrhhrrh) mouse. Invest Ophthalmol Vis Sci. 1988; 29:1190–1194. [PubMed: 2458328]
14. Ohnishi Y, Kohno T. Polychlorinated biphenyls poisoning in monkey eye. Invest Ophthalmol Vis Sci. 1979; 18:981–984. [PubMed: 113362]
15. Sullivan BD, Evans JE, Cermak JM, et al. Complete androgen insensitivity syndrome: effect on human meibomian gland secretions. Arch Ophthalmol. 2002; 120:1689–1699. [PubMed: 12470144]
16. Sullivan BD, Evans JE, Dana MR, Sullivan DA. Influence of aging on the polar and neutral lipid profiles in human meibomian gland secretions. Arch Ophthalmol. 2006; 124:1286–1292. [PubMed: 16966624]
17. Ding J, Kam WR, Dieckow J, Sullivan DA. The influence of 13-cis retinoic acid on human meibomian gland epithelial cells. Invest Ophthalmol Vis Sci. 2013; 54:4341–4350. [PubMed: 23722388]
18. Ding J, Sullivan DA. The effects of insulin-like growth factor 1 and growth hormone on human meibomian gland epithelial cells. JAMA Ophthalmol. 2014; 132:593–599. [PubMed: 24743973]

19. Kam WR, Sullivan DA. Neurotransmitter influence on human meibomian gland epithelial cells. Invest Ophthalmol Vis Sci. 2011; 52:8543–8548. [PubMed: 21969302]
20. Khandelwal P, Liu S, Sullivan DA. Androgen regulation of gene expression in human meibomian gland and conjunctival epithelial cells. Mol Vis. 2012; 18:1055–1067. [PubMed: 22605918]
21. Liu S, Hatton MP, Khandelwal P, Sullivan DA. Culture, immortalization, and characterization of human meibomian gland epithelial cells. Invest Ophthalmol Vis Sci. 2010; 51:3993–4005. [PubMed: 20335607]
22. Liu S, Kam WR, Ding J, et al. Effect of growth factors on the proliferation and gene expression of human meibomian gland epithelial cells. Invest Ophthalmol Vis Sci. 2013; 54:2541–2550. [PubMed: 23493293]
23. Liu Y, Kam WR, Ding J, Sullivan DA. Effect of azithromycin on lipid accumulation in immortalized human meibomian gland epithelial cells. JAMA Ophthalmol. 2014; 132:226–228. [PubMed: 24357250]
24. Liu Y, Kam WR, Ding J, Sullivan DA. Can tetracycline antibiotics duplicate the ability of azithromycin to stimulate human meibomian gland epithelial cell differentiation? Cornea. 2015; 34:342–346. [PubMed: 25611398]
25. Sullivan DA, Liu Y, Kam WR, et al. Serum-induced differentiation of human meibomian gland epithelial cells. Invest Ophthalmol Vis Sci. 2014; 55:3866–3877. [PubMed: 24867579]
26. Rosen ED, Spiegelman BM. PPARgamma: a nuclear regulator of metabolism, differentiation, and cell growth. J Biol Chem. 2001; 276:37731–37734. [PubMed: 11459852]
27. Fan W, Yanase T, Nomura M, et al. Androgen receptor null male mice develop late-onset obesity caused by decreased energy expenditure and lipolytic activity but show normal insulin sensitivity with high adiponectin secretion. Diabetes. 2005; 54:1000–1008. [PubMed: 15793238]
28. Hammarstedt A, Andersson CX, Rotter Sopasakis V, Smith U. The effect of PPARgamma ligands on the adipose tissue in insulin resistance. Prostaglandins Leukot Essent Fatty Acids. 2005; 73:65–75. [PubMed: 15936183]
29. Nien CJ, Massei S, Lin G, et al. The development of meibomian glands in mice. Mol Vis. 2010; 16:1132–1140. [PubMed: 20664693]
30. Nien CJ, Massei SR, Lin G, et al. Effects of age and dysfunction on human meibomian glands. Arch Ophthalmol. 2011; 129:462–469. [PubMed: 21482872]
31. Nien CJ, Paugh JR, Massei S, et al. Age-related changes in the meibomian gland. Exp Eye Res. 2009; 89:1021–1027. [PubMed: 19733559]
32. Jester BE, Nien CJ, Winkler M, et al. Volumetric reconstruction of the mouse meibomian gland using high-resolution nonlinear optical imaging. Anat Rec (Hoboken). 2011; 294:185–192. [PubMed: 21234992]
33. Lin CY, Suhalim JL, Nien CL, et al. Picosecond spectral coherent anti-Stokes Raman scattering imaging with principal component analysis of meibomian glands. J Biomed Opt. 2011; 16:021104. [PubMed: 21361667]
34. Brown DJ, Lin B, Holguin B. Expression of neuregulin 1, a member of the epidermal growth factor family, is expressed as multiple splice variants in the adult human cornea. Invest Ophthalmol Vis Sci. 2004; 45:3021–3029. [PubMed: 15326116]
35. Spirin KS, Ljubimov AV, Castellon R, et al. Analysis of gene expression in human bullous keratopathy corneas containing limiting amounts of RNA. Invest Ophthalmol Vis Sci. 1999; 40:3108–3115. [PubMed: 10586931]
36. Tontonoz T, Spiegelman BM. Fat and beyond: The diverse biology of PPARgamma. Ann Rev Biochem. 2008; 77:289–312. [PubMed: 18518822]
37. Trivedi NR, Cong Z, Nelson AM, et al. Peroxisome proliferator-activated receptors increase human sebum production. J Invest Dermatol. 2006; 126:2002–2009. [PubMed: 16675962]
38. Adams M, Reginato MJ, Shao D, et al. Transcriptional activation by peroxisome proliferator-activated receptor gamma is inhibited by phosphorylation at a consensus mitogen-activated protein kinase site. J Biol Chem. 1997; 272:5128–5132. [PubMed: 9030579]
39. Hu E, Kim JB, Sarraf P, Spiegelman BM. Inhibition of adipogenesis through MAP kinase-mediated phosphorylation of PPARgamma. Science. 1996; 274:21003.

40. Geiss-Friedlander R, Melchior F. Concepts in sumoylation: a decade on. Nat Rev Mol Cell Biol. 2007; 8:947–956. [PubMed: 18000527]
41. Burgemeister I, Seger R. MAPK kinases as nucleo-cytoplasmic shuttles for PPARg. Cell Cycle. 2007; 6:1539–1548. [PubMed: 17611413]
42. van Beekum O, Fleskens V, Kalkhoven E. Post translational modifications of PPAR-gamma: fine-tuning the metabolic master regulator. Obesity (Silver Spring). 2009; 17:213–219. [PubMed: 19169221]
43. Makrantonaki E, Zouboulis CC. Testosterone metabolism to 5a-dihydrotestosterone and synthesis of sebaceous lipis is regulated by the peroxisome proliferator-activated receptor ligand linoleic acid in human sebocytes. Br J Dematol. 2007; 156:428–432.
44. Wrobel A, Seltmann H, Fimmel S, et al. Differentiation and apoptosis in human immortalized sebocytes. J Invest Dermatol. 2003; 120:175–181. [PubMed: 12542519]
45. Xia L, Zouboulis CC, Ju Q. Culture of human sebocytes in vitro. Dermatoendocrinol. 2009; 1:92–95. [PubMed: 20224690]
46. Zouboulis CC, Seltmann H, Neitzel H, Orfanos CE. Establishment and characterization of an immortalized human sebaceous gland cell line (SZ95). J Invest Dermatol. 1999; 113:1011–1020. [PubMed: 10594745]
47. Robertson DM, Li L, Fisher S, et al. Characterization of growth and differentiation in a telomerase-immortalized human corneal epithelial cell line. Invest Ophthalmol Vis Sci. 2005; 46:470–478. [PubMed: 15671271]

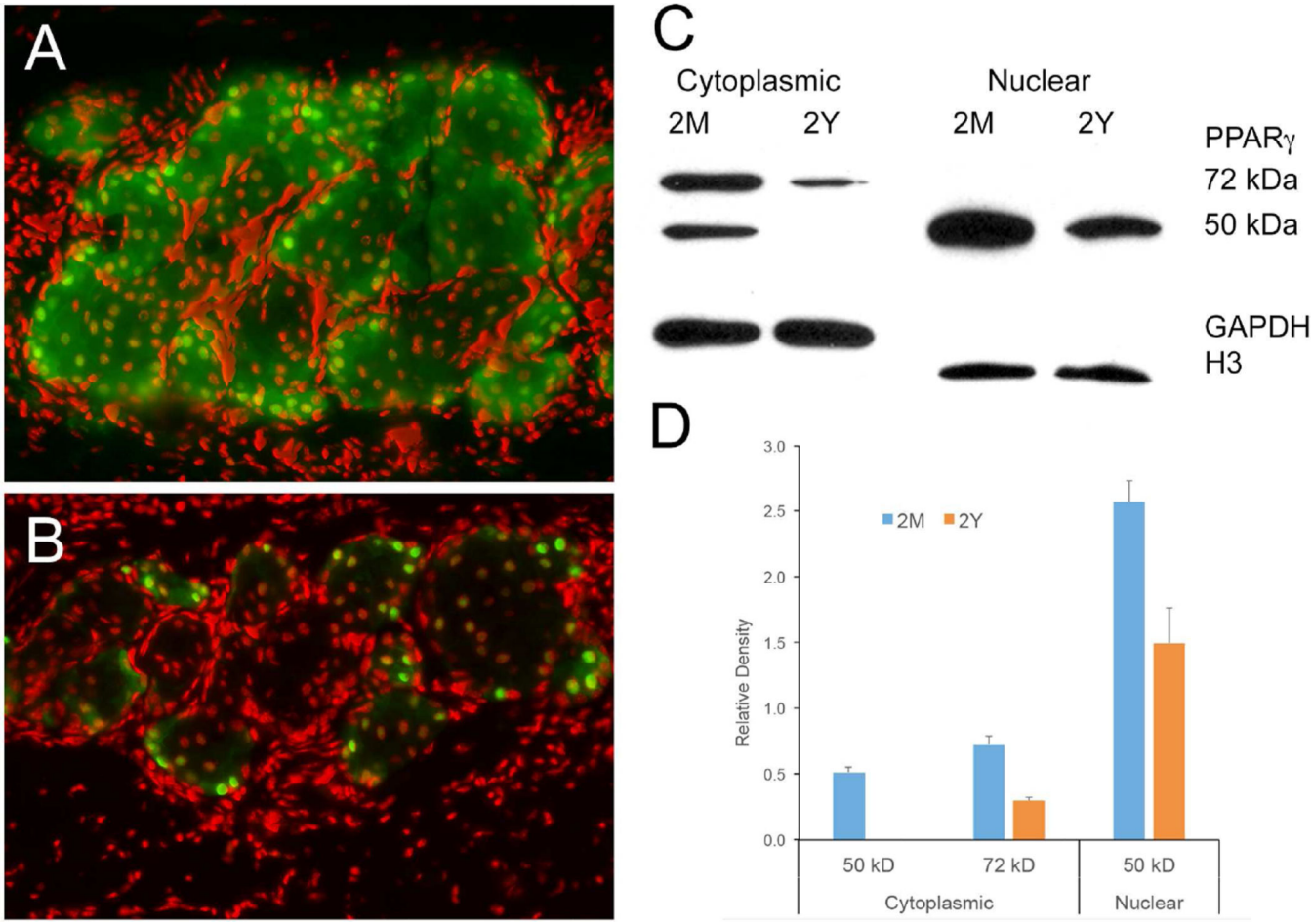

Figure 1.

PPARγ localization in mouse meibomian gland identified by immunostaining (A and B) and western blotting (C and D) (Representative of 3 mice per age for immunocytchemistry and pooled meibomian gland proteins from 5 mice for each age). Young mice (A) showed both nuclear and cytoplasmic PPARγ staining while old mice (B) showed predominantly nuclear staining (green = PPARγ, red = nuclei). Western blots (C) and densitometry averaged from 3 western blots and normalized using GAPDH for cytoplasmic fraction and Histone 3 for nuclear fraction (D) show that the nucleus contains only the 50 kDa PPARγ band which is significantly ($P<.05$) reduced in old mice, while the cytoplasmic fraction shows loss of the 50 kDa band and a significantly ($P<.05$) reduced 72 kDa PPARγ band in old glands (error bar = standard deviation).

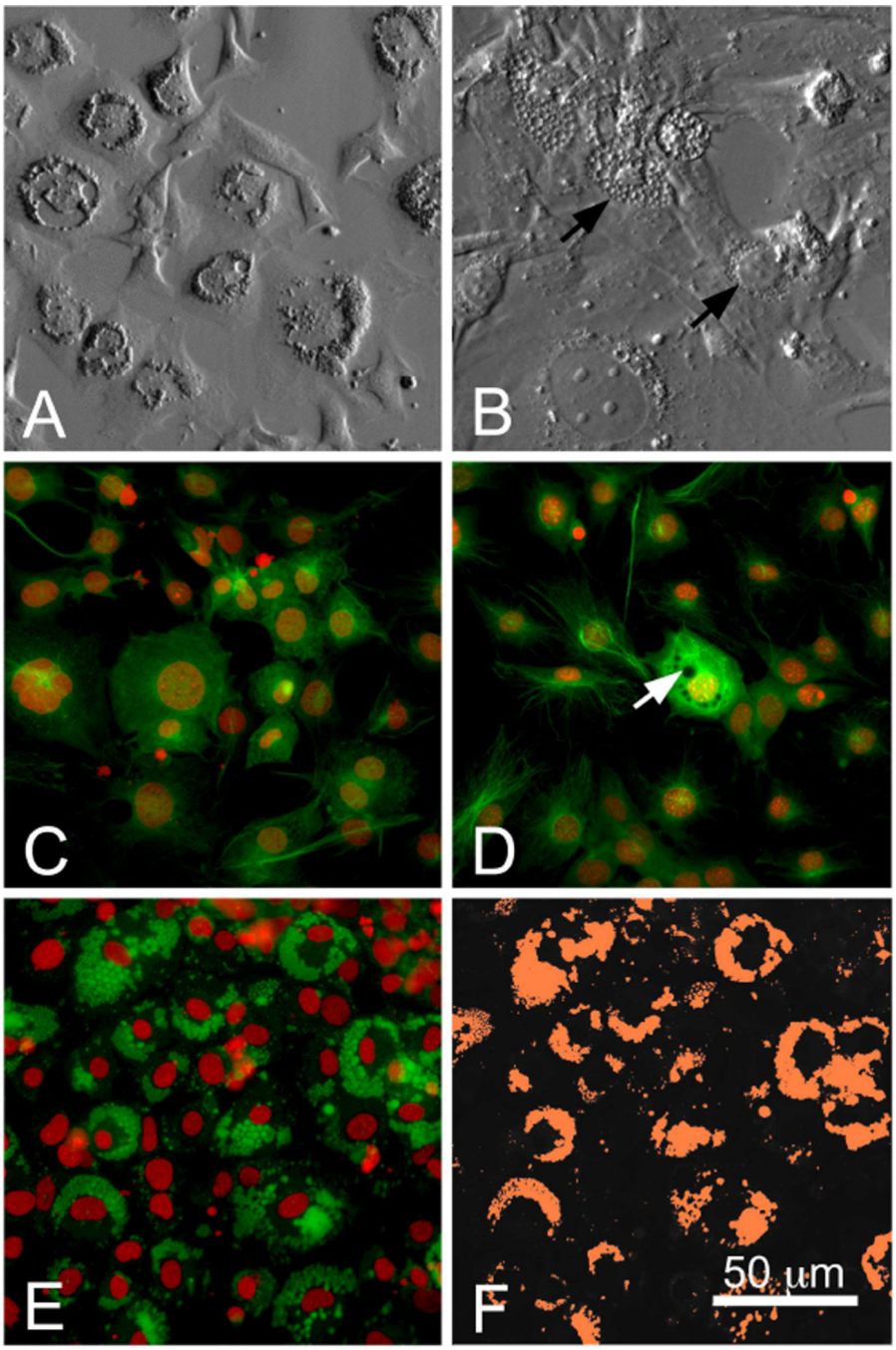

Figure 2.

Brightfield (A and B) and PPARγ immunostaining (C and D) of primary cultured mouse meibocytes (A and C) and SV40 immortalized CN-G2 meibocytes (B and D). Note that both cells in culture appear to contain prominent vacuoles (arrows) and show cyotplasmic and nuclear PPARγ staining. Cytoplasmic vacuoles showed strong staining with fluorescent LipidTox (E) indicating the presence of neutral lipids. Area of LipidTox staining was then thresholded (F, orange area) to measure lipid area. Each image is representative of 3 separate coverslips.

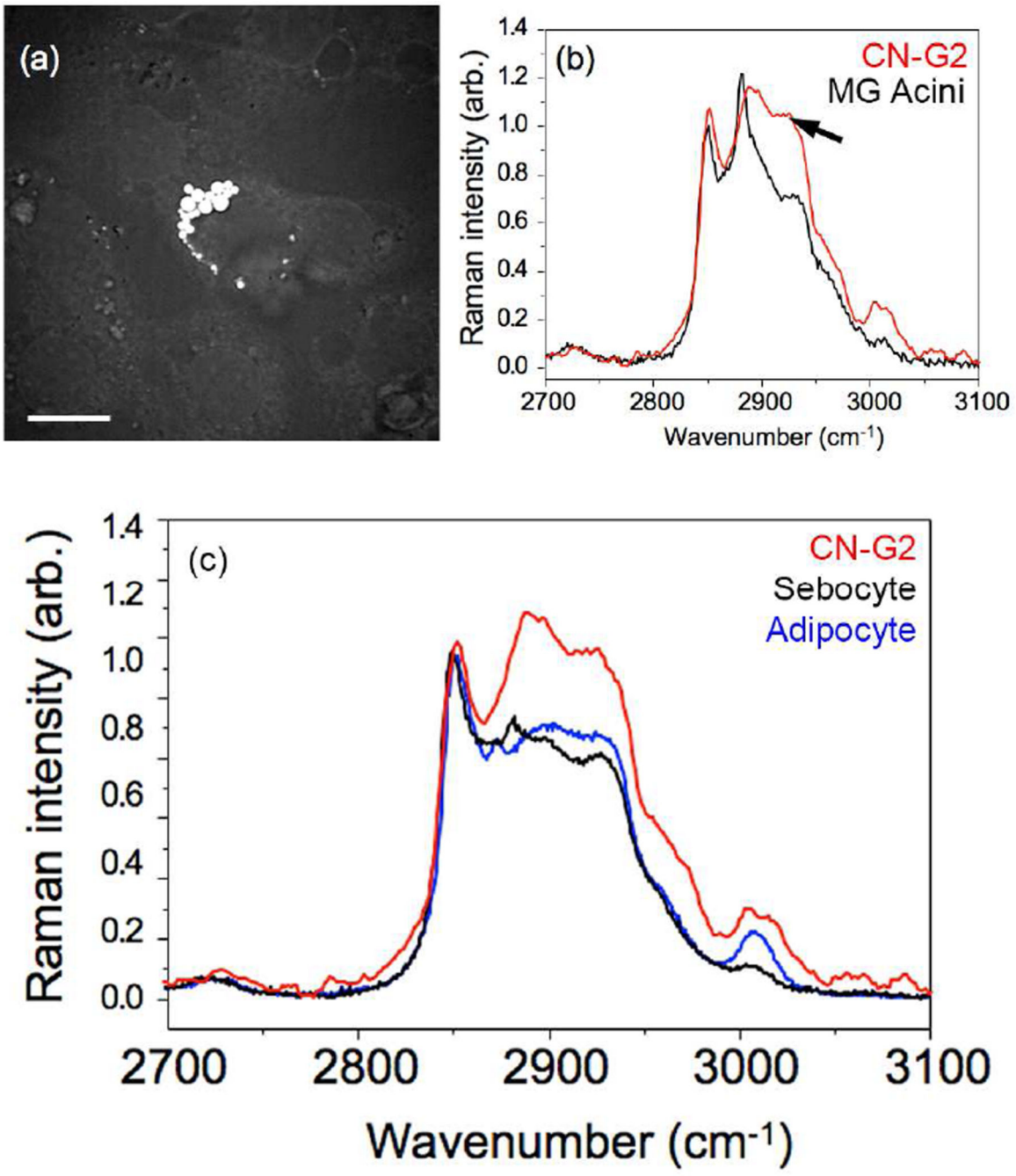

Figure 3.

Coherent Anti-Stokes Raman (CARS) image focused on 2845 cm^{-1} (A) and Raman microspectroscopy (B and C) of CN-G2 lipid vacuoles. CN-G2 cells (B and C, Red line) show major peaks at 2846 cm^{-1} and 2886 cm^{-1}, similar to that of lipid within meibomian gland acini (B) indicating the abundance of wax and cholesterol esters, respectively. Lipid in CN-G2 cells was distinct from that of lipid within sebocytes and adipocytes (C, black and blue, respectively), which contain reduced cholesterol esters. Also note the presence of an elevated peak at 2940 cm^{-1} from the CH_3 stretch region representative of protein in CN-G2

cells (B, arrow) that is also present in acinar lipid at reduced levels that show maturational changes within the meibomian gland lipid.

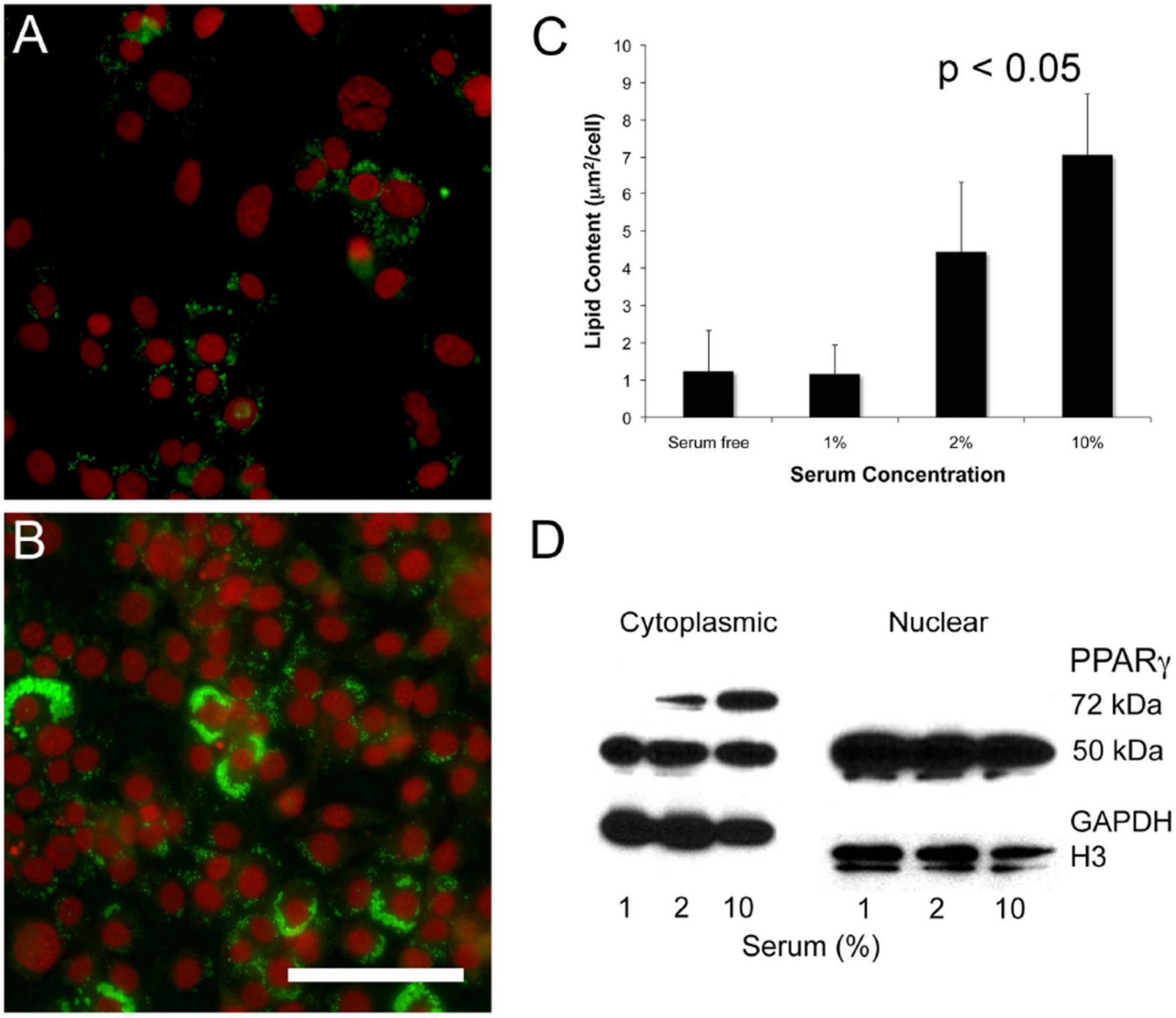

Figure 4.

Effects of serum on lipid synthesis (A-C) and PPARγ localization (D) in CN-G2 cells. CN-G2 cells grown in 0% serum media (A) showed reduced LipidTox staining compared to cells grown in 10% serum containing media (B; green = LipidTox, red = nuclei). Quantification of lipid area (C) showed that cells grown in 10% serum synthesized significantly more lipid than cells grown in reduced serum ($P<.05$). Fractionation of cells into the cytoplasmic and nuclear compartment showed that serum starved cells contained a signficiantly ($P<.05$) reduced amounts of 72 kDa PPARγ protein, with little change in the nuclear compartment. Western blot is representative of 3 separate experiments.

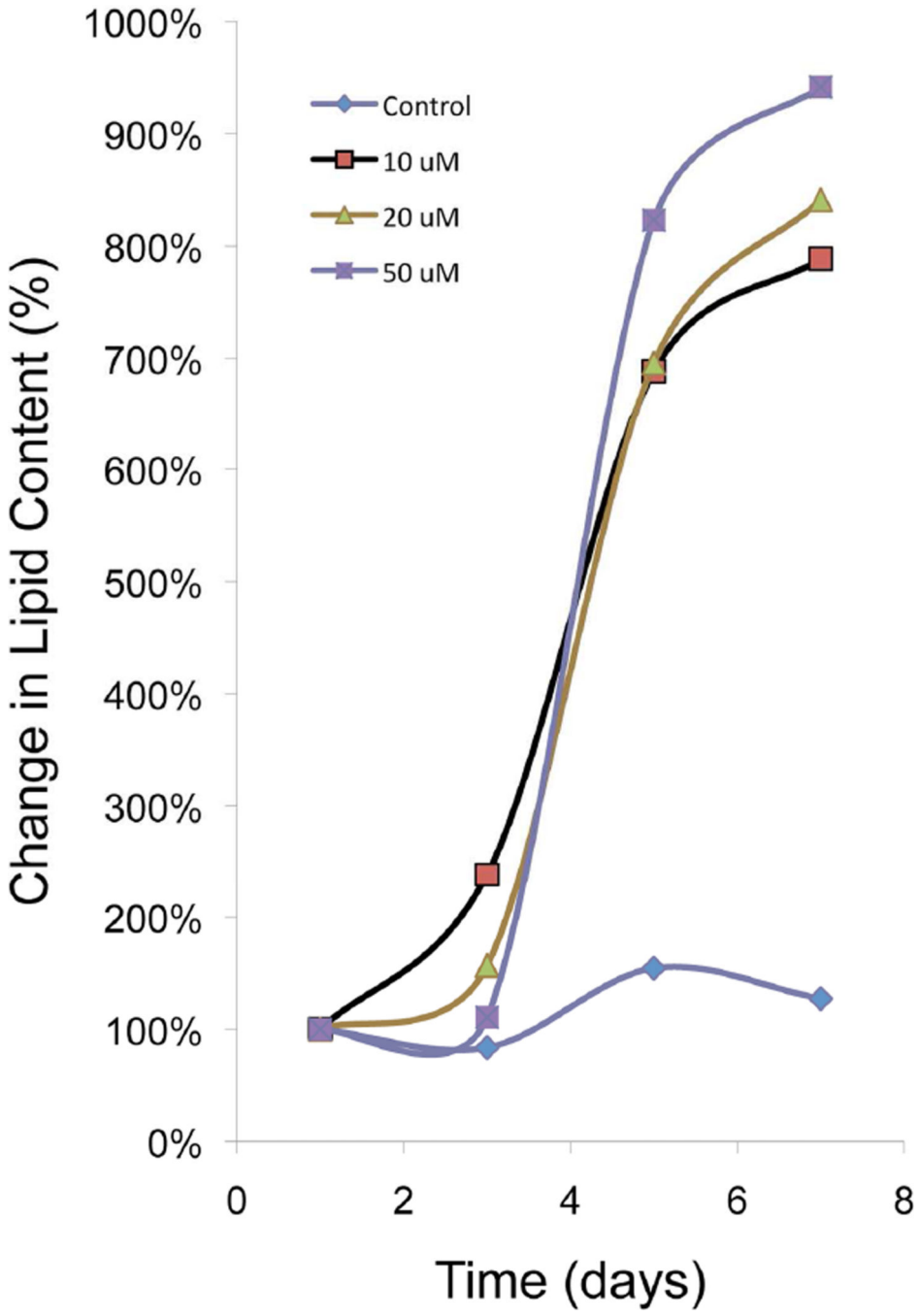

Figure 5.

Effects of 0, 10 μM, 20 μM, and 50 μM rosiglitazone on lipid synthesis in CN-G2 cells. Note that rosiglitazone dose and time-dependently stimulated a significant ($P<.05$), 8–10 fold increase in lipid area within CN-G2 cells. (Data is representative of 3 separate experiments).

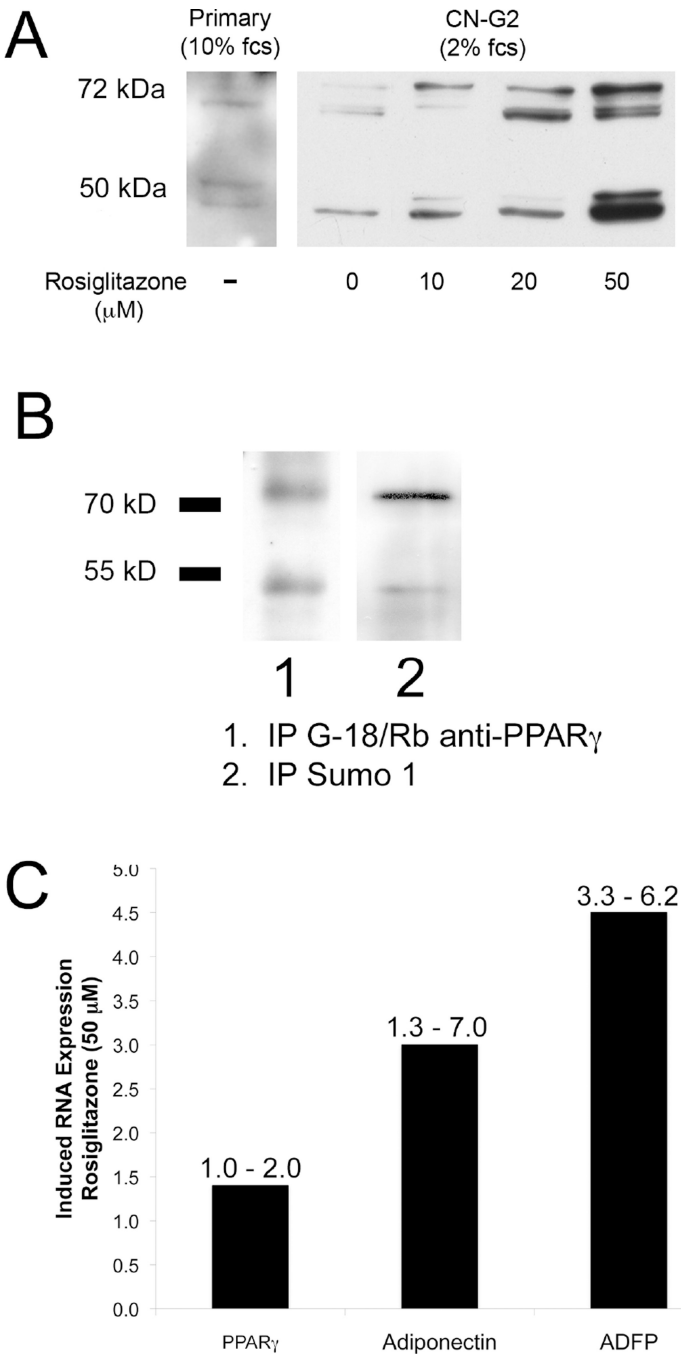

Figure 6.

Effects of rosiglitazone on PPARγ localization (A), post translational modification (B) and PPARγ response gene expression (C). Induced lipid synthesis by rosiglitazone was associated with a significant (P<.05) increase in cytoplasmic localization of PPARγ proteins showing multiple bands consistent with post translational modification involving serine phosphorylation and sumoylation (A). Immunoprecipitation of PPARγ using goat anti-PPARγ antibodies pulled down both the 50 kDA and 72 kDa proteins (B, Lane 1). Stripping and re-probing of western blot using a rabbit anti-SUMO1 antibody showed staining of the

72 kDa band, indicating sumoylation. Rosiglitazone also enhanced expression of PPARγ and other PPARγ response genes, adiponectin and ADFP (C).